Available online at www.sciencedirect.com
SCIENCE DIRECT®
Mechanics of Materials 36 (2004) 45–55
MECHANICS OF MATERIALS
www.elsevier.com/locate/mechmat

Thermal cycling response of layered gold/polysilicon MEMS structures

Ken Gall *, Martin L. Dunn, Yanhang Zhang, Brian A. Corff

Department of Mechanical Engineering, University of Colorado at Boulder, Boulder, CO 80309, USA

Received 8 January 2002; received in revised form 17 May 2002

Abstract

Multi-layer material structures in micro-electromechanical systems (MEMS) differ considerably from their microelectronic counterparts since the thicknesses of the film and substrate are comparable. Due to thermal expansion coefficient mismatch between metallic and polysilicon materials, thermal fluctuations in multi-layer MEMS structures may lead to out of plane displacements several times the structure thickness. In the present study we examine the deformation of a series of gold/polysilicon test structures produced using the commercial multi-user MEMS Process. The test structures are multi-layer plates with a gold layer that is 0.5 μm thick on a polysilicon layer with a thickness that is either 1.5 or 3.5 μm. The structures have varying in-plane dimensions on the order of 50–300 μm. Using an interferometric microscope, we measure the full-field deformed shapes of the Au–Si structures subjected to thermal cycles or hold periods. Depending on the Au–Si plate geometry, the structures deform in a non-linear manner and buckle when the temperature change is large enough. When subjected to temperature holds, the curvature of the plates relaxes. Beam-like plates subjected to repeated thermal cycles demonstrate a cyclic response that depends strongly on the mean (or maximum) temperature. Samples cycled at lower mean temperatures show significant ratcheting toward lower curvatures as the number of cycles approaches 10,000. Samples cycled at higher mean temperatures undergo degradation of surface reflectivity as the number of cycles approaches 1000.

1. Introduction

Emerging micro-electromechanical systems (MEMS) contain ever-increasing levels of complexity including moving mechanisms, contacting parts, and layered material systems. For example, Fig. 1 shows a bimorph micro-switch actuator comprised of a thin gold (Au) film deposited on a thin polysilicon (Si) film (Miller et al., 2001). The actuator functions electrostatically, but the curvature observed in the beam is due to the thermal expansion coefficient mismatch between the two material layers in the multi-layer system and is very similar to that observed in the beams used in this study. Aside from switching, numerous other structural roles can be served by the use of multi-layer material systems in MEMS such as actuation or surface shaping. Although the use of multi-layer material systems in MEMS introduces a design

* Corresponding author. Tel.: +1-303-735-2711; fax: +1-303-492-3498.
E-mail address: kgall@colorado.edu (K. Gall).

0167-6636/$ - see front matter © 2003 Elsevier Ltd. All rights reserved.
doi:10.1016/S0167-6636(03)00030-9

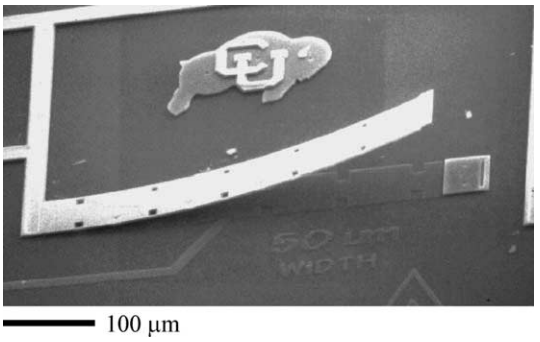

Fig. 1. SEM image of a Au–Si bimaterial beam used in a MEMS switch (Miller et al., 2001).

degree of freedom, their use also admits unique material behavior and reliability issues and requires the use of advanced science and engineering design tools.

Multi-layer material systems consisting of thin films deposited on thick substrates have been extensively studied in the micro-electronics sector. Specifically, the thermomechanical behavior of thin metal films deposited on relatively thick rigid substrates such as silicon has received considerable attention in the past (e.g. Nix, 1989). Much work in this area focused on understanding the stresses in thin films using wafer curvature measurements and the Stoney formula (Stoney, 1909). Subsequent work has focused on the thermomechanical behavior of thin films under repeated thermal cycles (Thouless et al., 1993; Shen and Suresh, 1995; Evans et al., 1997; Koike et al., 1998; Harris and King, 1998; Keller et al., 1999; He et al., 1997; Leung et al., 2000). The aforementioned studies have placed particular emphasis on understanding the micro-mechanisms that lead to the overall deformation response and subsequent evolution and degradation during thermal cycling.

The overall thermomechanical response of thin metallic films on thick substrates subjected to thermal fluctuations is reasonably well established. For systems in which the thermal expansion coefficient of the film is greater than that of the substrate, the thin metallic films usually have a residual tensile stress at room temperature created by cooling the multi-layer system from a higher processing temperature—the metallic layer typically attempts to contract more than the substrate. If the multi-layer structure is heated from room temperature, the tensile stresses will initially decrease linearly towards a compressive regime. Upon continued heating, the slope of the stress–temperature response decreases, and the stress approaches zero at high temperatures. Upon subsequent cooling the stress–temperature response follows a path such that the overall response demonstrates a closed hysteresis in stress–temperature space. If irreversible micro-structural changes occur, the hysteresis loop will often not close, particularly during the first thermal cycle. The inelastic deformation mechanisms controlling the aforementioned non-linear thermomechanical response have been a subject of some discussion. Numerous inelastic deformation mechanisms have been reported and wrapped into modeling efforts such as temperature dependent dislocation motion (Nix, 1989), grain-boundary diffusion (Thouless et al., 1993), and power-law creep (Keller et al., 1999).

Due to the transfer of standard batch fabrication processing practice from integrated circuits, thin metallic films in MEMS components often share the same initial micro-structure as their electronic counterparts. However, the substrate in multi-layer MEMS structures has a thickness on the order of the film itself in contrast to thin films in micro-electronics which are typically deposited on substrates hundreds of times thicker than the film. The difference in the substrate thickness between MEMS and micro-electronics applications leads to quite different behavior during thermomechanical loading. Some representative differences are listed below:

1. During thermal cycling, MEMS structures experience out-of-plane displacements several orders of magnitude larger than their micro-electronic counterparts. As a result, MEMS structures can exhibit geometric non-linearity and bifurcation during thermal loading. Moreover, changing the relative thickness of the film/substrate system significantly alters the stress-state and degree of non-linearity. Understanding these bifurcations and non-linearities is critical in developing the tools to tailor the

geometry (size and thickness) of MEMS structures and produce useful micro-systems.
2. Since the material layers in MEMS structures are of comparable thickness, significant stress and strain gradients can exist through the thickness of the films. These stress gradients make it difficult to use an average stress metric to characterize the loading state.
3. The coupling between the applied temperature range and the induced stress level differs considerably in MEMS structures compared to micro-electronics. This difference has ramifications on the operant degradation modes during creep and fatigue. For example, the thermomechanical fatigue of films in micro-electronics has been limited to the extreme low cycle regime for typical temperature cycles (Thouless et al., 1993). For equivalent temperature changes, thin films in MEMS structures will experience lower stress values and higher cycle numbers. Understanding the difference in the micro-mechanisms of low and high cycle fatigue in the films is imperative. An equivalent argument exists for the mechanisms of creep deformation.

Based partially on the differences noted above, it is clear that the research efforts completed in the micro-electronics arena will not directly transfer to multi-layer MEMS structures. Work is in progress by several researchers to study the monotonic and cyclic deformation mechanisms in metallic thin films relevant to MEMS. Some examples are the study of the geometric non-linearity in thin film/substrate structures (Salamon and Masters, 1995; Finot and Suresh, 1996; Freund, 2000; Dunn et al., 2001), the fatigue of freestanding thin films (Read, 1998; Schwaiger and Kraft, 1999), creep of multi-layer MEMS structures (Zhang and Dunn, 2001), and the cyclic deformation of thin film/substrate systems (Hommel et al., 1999). Much of the experimental work presented above is preliminary in nature and often focuses on a particular material such as silver, copper, or gold. The measurement technique also differs considerably depending on the investigator, ranging from micro-beam deflection (Schwaiger and Kraft, 1999) to miniature tensile testing configurations (Read, 1998).

In the present paper we study the deformation of a commercially available MEMS material system, Au–Si. The test structures consist of 0.5 μm of Au deposited on 1.5 or 3.5 μm of polysilicon. Full-field deflections of Au–Si beams and plates subjected to temperature changes are measured in situ using interferometric microscopy. The purpose of this investigation is to evaluate the deformation patterns of the Au–Si test structures under monotonic and cyclic temperature changes and hold periods. We begin by outlining the materials and experimental methods employed. Following this, we present the experimental measurements in various forms. The experimental results are then discussed in light of previous work and future work is delineated. The paper ends with conclusions.

2. Materials and methods

The gold/polysilicon beam and plate microstructures were fabricated using the commercially available multi-user MEMS process (MUMPs, Koester et al., 2001). The so-called surface micromachining process consists of a series of standard micro-electronics lithography, thin-film deposition, and etching processes. Briefly, the relevant steps of the complete process consist of depositing a 2 μm thick sacrificial film of phosphosilicate glass (PSG) on top of a 600 nm thick silicon nitride film on a (1 0 0) single crystal silicon wafer by low pressure chemical vapor deposition. A 2 μm thick polysilicon film (Poly 1) is then deposited on the PSG, patterned, and etched. A second PSG film 200 nm thick is then deposited and the wafer is annealed to dope the polysilicon with phosphorus from both PSG films, and to reduce the residual stress in the polysilicon film. The top PSG and polysilicon films are lithographically patterned and etched to produce the desired beam and plate shapes and sizes. Another 0.75 μm thick PSG film is then deposited, followed by a second 1.5 μm thick polysilicon film (Poly 2), and another 200 nm PSG film to serve as a mask for patterning and etching the Poly 2 layer to conform to the desired beam and plate shapes and sizes. This is followed by another annealing process to minimize residual

stresses and stress gradients. A 0.5 μm gold film with a very thin chromium adhesion layer is deposited, then lift-off patterned. Finally, the polysilicon/gold micro-structures are freed from the substrate by etching away the first PSG film in a 49% hydrofluoric acid solution. In order to assure the etchant attacks the PSG completely and in a timely manner, etch holes are patterned in the micro-structures to provide an easy flow path for the etchant.

Representative plate (300 μm by 300 μm) and beam (50 μm by various lengths up to 340 μm) structures are shown in Fig. 2. The structures in Fig. 2 were imaged by a scanning electron microscope (SEM). A support post exists at the center of the plates and beams to secure the structure to the base Si wafer, and allow them to deform as freely as possible under a temperature change. The structures initially contain PSG between the Au–Si plate and the nitride layer on the Si base wafer. The PSG is removed in a standard release process that consists of submersing the structure in HF acid for 4.5 min followed by drying in a CO_2 critical point dryer. The etch holes dispersed throughout the plates and beams in Fig. 2 allow etchant to reach the PSG beneath the plate during the release of the structure. The Au layer is always 0.5 μm while the polysilicon layer is either 1.5 or 3.5 μm. The outer dimensions of the structures vary, as shown in Fig. 2.

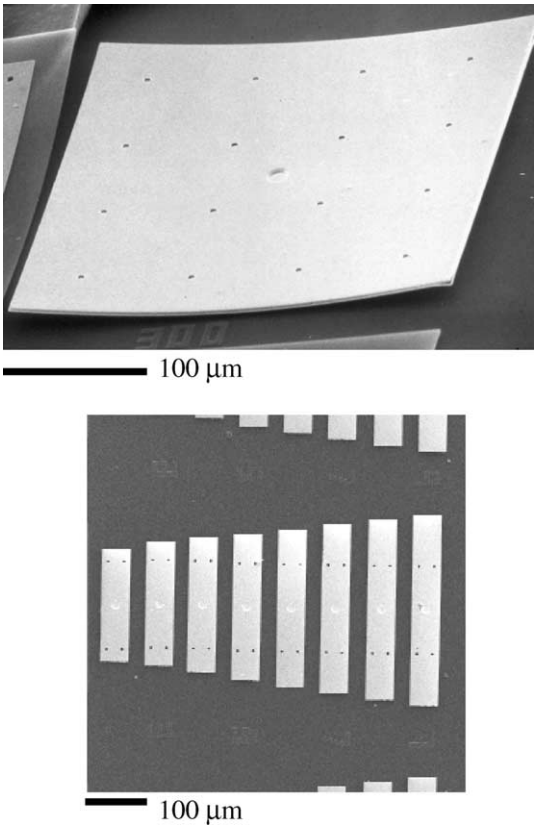

Fig. 2. SEM images of plate (top) and beam (bottom) Au–Si test structures.

The as-fabricated micro-structure of the Au layer was investigated by employing a focused ion beam (FIB) microscope. The FIB can be used to make cross-sectional cuts through a structure and to subsequently image the sliced materials. Imaging in a FIB differs from that of a SEM in that the specimen is bombarded with ions, which can preferentially attack certain regions in the sample, such as grain boundaries, specific crystal orientations, or phases. We performed several cuts through the multi-layer MEMS test structures shown in Fig. 2. Fig. 3a presents a low magnification image of a square FIB cut made in the edge of a round as-released plate. Fig. 3b is a close-up view of the cross-section through the plate showing the different materials present. The scale in the horizontal and vertical directions in Fig. 3a and b differs because the sample is tilted 45° in the stage. In Fig. 3b, the grain structure is apparent. The grain size of the as-released polycrystalline Au film is generally smaller than the film thickness. This observation is consistent with findings on as deposited films in micro-electronics.

Individual MEMS chips, which may contain as many as 50 test structures, are subjected to thermal fluctuations in a special thermal chamber with a temperature range of −190 to 600 °C. The chamber has controllable heating and cooling rates so that specific cycle blocks can be applied in a timely manner. Fig. 4 is a plot of the temperature in the chamber as a function of time for a representative thermal cycling experiment. Small hold periods, which result in the stair–step pattern of the temperature profile shown in Fig. 4, were necessary for in situ displacement measurements. Measurements

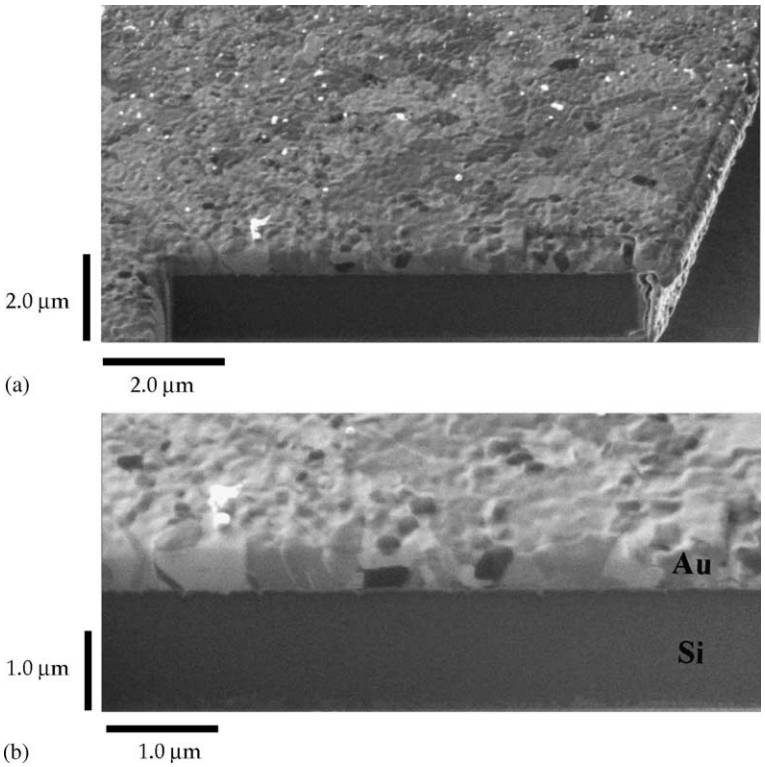

Fig. 3. FIB image of the micro-structure of 0.5 μm Au deposited on 1.5 μm of Si shown at (a) low and (b) high magnifications in a cross-section cut through a plate structure. The Au and Si materials are marked on image (b). The scale in the horizontal and vertical directions differs because the sample is tilted 45°.

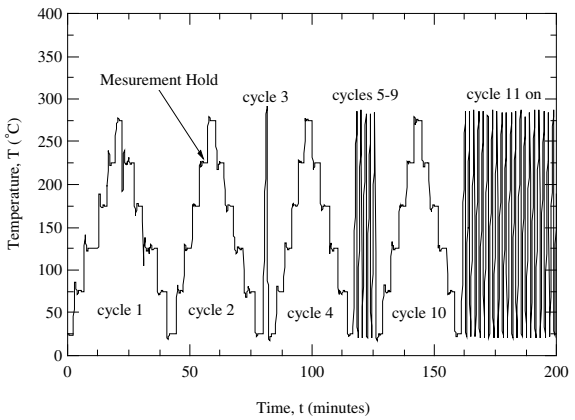

Fig. 4. Thermal cycling profile within the temperature chamber. The steps represent hold periods where measurements were taken with the interferometric microscope.

were only made at certain cycle intervals to minimize possible hold time effects.

During heating or cooling, the full-field displacement of selected plate structures is measured in situ using an interferometric microscope. The out-of-plane displacement resolution of the microscope is on the order of nm, and the viewing window is approximately one square mm, allowing measurement to occur simultaneously on several MEMS test structures. The measurements rely upon a surface that is relatively smooth and normal to the objective lens. If the sample curves significantly and the slope of the displacement field is too large, or excessive surface roughening is encountered, measurements cannot be made. The microscope provides raw data in the form of height versus in-plane position. Using this information, the curvature, κ, for selected linear paths can be calculated. Data throughout the paper will

be presented as either raw height data or the curvature of specimens at specific temperatures.

Finite element modeling was completed with ABAQUS, and details can be found in Dunn et al. (2002). The model used composite shell elements to approximate the thin-plate kinematics of the Kirchoff theory. Geometric non-linearity is modeled using the well-known von Karman theory for thin plates with large deflections. Both materials are modeled as linear elastic with isotropic material properties. Input parameters to the finite element calculations are $E_2 = 163$ GPa, $v_2 = 0.22$ $E_1 = 78$ GPa, $v_1 = 0.42$. The thermal expansion coefficients of the materials were assumed to vary linearly with temperature and values at 100(24) °C used are $\alpha_2 = 3.1(2.6) \times 10^{-6}$ °C^{-1}, and $\alpha_1 = 14.6(14.2) \times 10^{-6}$ °C^{-1}. Typical finite element meshes for the plate micro-structures contained elements with a characteristic dimension of about 12.5 μm, a size that was chosen after a convergence study with mesh size.

3. Results

The experimental and modeling results are presented in Figs. 5–12. Fig. 5 presents a series of deformed shapes as a function of temperature for a 300 μm by 50 μm beam that has been thermally cycled 100 times from −50 to 200 °C, prior to this particular measurement. The out-of-plane displacements are magnified by a factor of 50 to visualize the dependence of the beam curvature on temperature. At low temperatures, the beam curves upwards away from the substrate due to the larger contraction of the Au layer compared to the polysilicon layer. For this sample and temperature cycling range, the beam ends are no longer measurable below about 80 °C due to large slope of the beam. However, the center portion of the curved beam that remains in focus can still be used to determine the overall curvature of the beam. As the temperature is raised, the curvature of the beam decreases as the Au expands more than the Si substrate. Towards higher temperatures, the curvature eventually reverses itself away from the microscope (Fig. 5).

The series of images in Fig. 5 were created using actual displacement data, and they provide a good visualization tool for the overall thermomechanical response. A more quantitative and compact representation of the data in Fig. 5 is average curvature versus temperature plots (Figs. 6 and 7). In Figs. 6 and 7 we plot curvature along the long

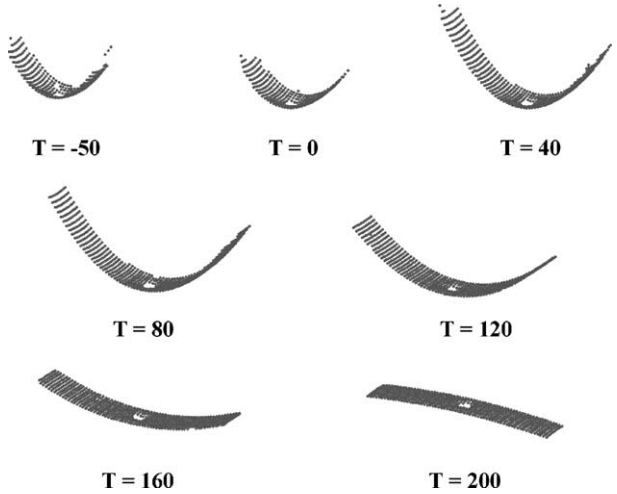

Fig. 5. Example of a typical surface plot reproduction created using the full-field displacement data for the 300 μm by 50 μm beam during cycle number 100. Temperature is in °C. The curvatures are exaggerated by increasing the scale in the plane of the beam by 50 times. Below 80 °C the ends of the beam are not visible by interference patterns because the displacement is too large.

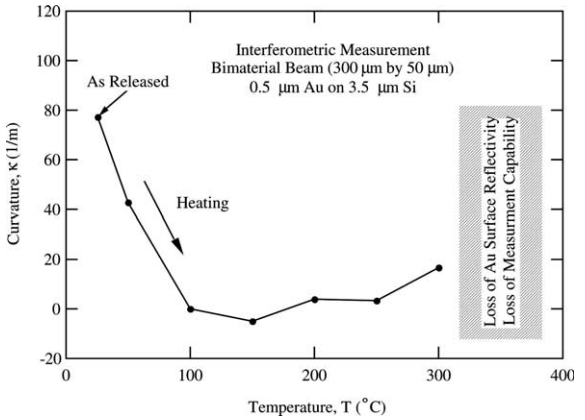

Fig. 6. Curvature–temperature response of an as-released beam heated until the specimen reflectivity degraded to the point that measurements could no longer be obtained with the interferometric microscope.

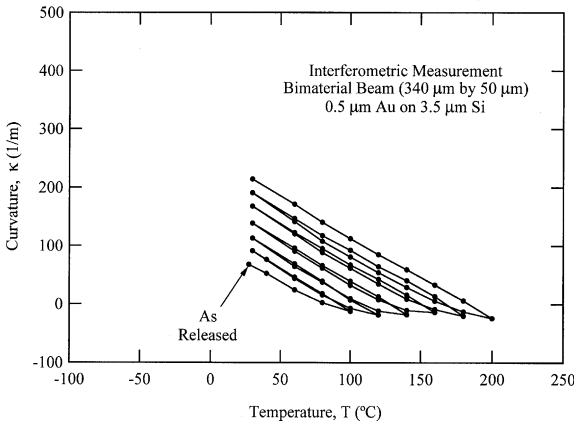

Fig. 7. Curvature–temperature response of an as-released beam cycled in an incremental step pattern for continuously increasing temperatures.

axis of a beam as a function of temperature. The measurement begins at room temperature (25 °C) on an as-released sample and the temperature is raised monotonically while incremental curvature measurements are made. As observed in Fig. 5, the curvature decreases towards a negative value as the temperature increases. The curvature has a tendency to saturate around 200 °C, and increases as the temperature is subsequently raised towards 300 °C. Above 300 °C the Au surface reflectivity degrades severely and interference measurements on the Au surface become impractical (Burns and Bright, 1998). A similar response is shown in Fig. 7, with the exception that the change in temperature (ΔT) is incrementally increased and decreased. The incremental unloading response shows that the Au–Si structures exhibit a significant dependence on the maximum temperature experienced during a cycle from the as-released state. The slope of the curvature temperature response is independent of the maximum temperature, however, the maximum curvature developed upon cooling increases as the maximum temperature increases. The results indicate a permanent strain in the Au with an accompanying inelastic deformation mechanism. Complete details of this response are given by Zhang and Dunn (2003).

Certain Au–Si multi-layer structures demonstrate a non-linear thermomechanical response. Fig. 8 plots average specimen curvature as a function of temperature for square plates of various sizes. The experimental data in Fig. 8a was taken on as-released plates that were cycled from room temperature to 100 °C several times and then cooled to room temperature. It is important to understand that the response of the plates in Fig. 8 was tracked *after* applying about three thermomechanical cycles to temporarily *stabilize* the thermomechanical response in this temperature range. The modeling data in Fig. 8b was constructed using a multi-layer finite element model that accounts for geometric non-linearity (Dunn et al., 2002). Curvatures in the x-direction, κ_x, and curvature in the y-direction, κ_y, are presented in both Fig. 8a and b. For all of the plates, the curvature–temperature relationship is linear at small curvatures and non-linear at large curvature values. Moreover, the results in Fig. 8 show a plate size dependence of the curvature–temperature relationship. Upon the same thermal loading, larger plates tend to resist deformation and even show a bifurcation of the curvatures in the x and y directions. Smaller plates curve more readily into a spherical deformation pattern. The modeling results capture the overall trends of the experimental measurements including the bifurcation in the larger plate.

The Au–Si plates were found to experience creep if held at a constant temperature for a period of time. In Fig. 9 we present curves of curvature

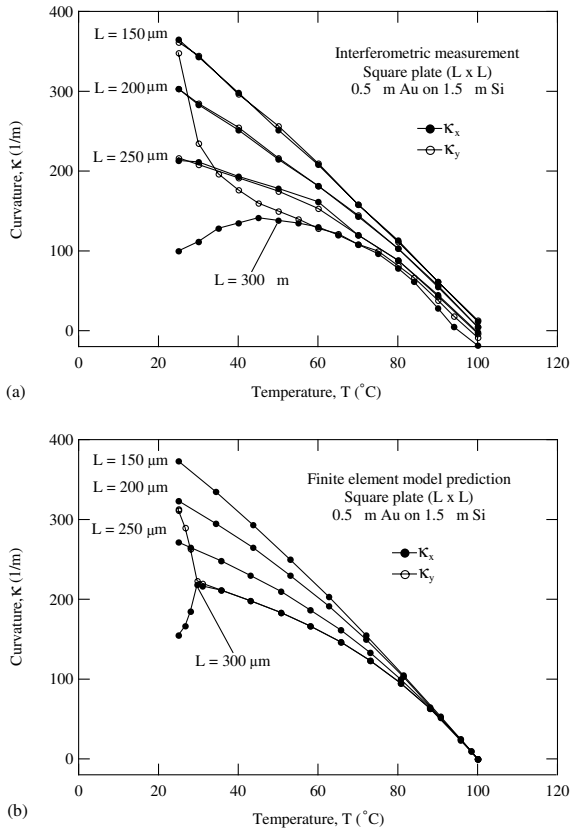

Fig. 8. (a) Experimentally measured and (b) predicted curvature versus temperature plots for plates of various sizes.

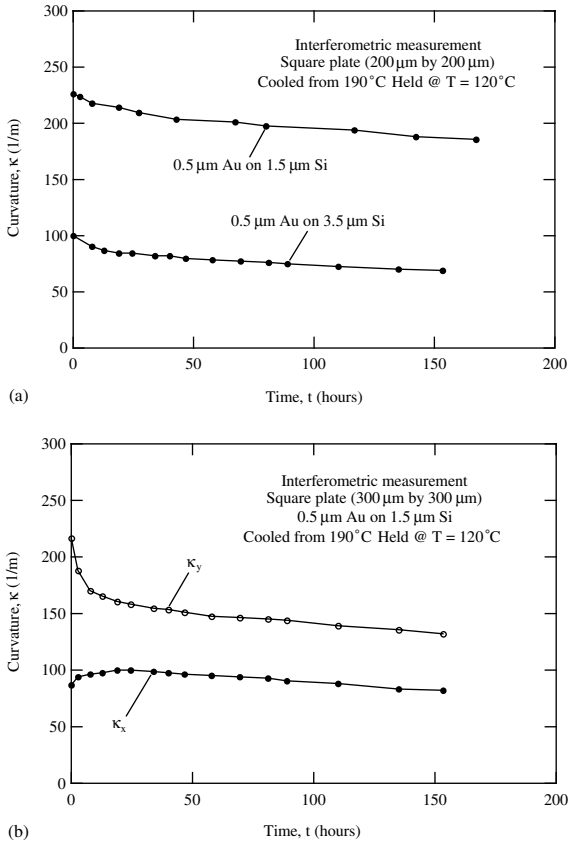

Fig. 9. Creep behavior of (a) 200 μm symmetric and (b) 300 μm buckled plate structures.

versus hold time for 200 μm square plates (Fig. 9a) and 300 μm square plates (Fig. 9b) held at 120 °C. The larger plates are buckled in their initial configuration, while the smaller plates are deformed spherically. Before experiencing the temperature hold, the as-released plates were heated from room temperature to 190 °C and subsequently cooled to 120 °C. In Fig. 9a we observe the creep behavior for 0.5 μm Au on 1.5 and 3.5 μm of Si, which both demonstrate a decrease in curvature as a function of time. The specimen with the thinner Si layer begins with a larger initial curvature, however, the creep rate of both specimens appears comparable. The buckled plate (Fig. 9b) shows an increase/decrease in the curvature in the x-direction, κ_x, and a decrease in the curvature in the y-direction, κ_y, over time. The creep curves in Fig. 9 for all plates show rates that are initially larger than the apparent steady-state rates. Complete details are given in Zhang and Dunn (2001).

The effect of repeated thermomechanical cycles is presented in Figs. 10–12. In Fig. 10 the temperature was cycled over a range of $\Delta T = 250$ °C and a mean temperature of $T_m = 75$ °C, where $\Delta T = T_{max} - T_{min}$ and $T_m = (T_{max} + T_{min})/2$. The 300 μm by 50 μm beam (Fig. 10a) and 200 μm by 50 μm beam (Fig. 10b) show nearly identical responses up to 100 cycles in contrast to the different size plate structures in Fig. 8, which showed a plate size dependence. The results in Fig. 10 show that the thermomechanical response is stable up to 100 cycles for $\Delta T = 250$ °C and $T_m = 75$ °C. Fig. 11 shows the effect of increasing $T_m = 75$–150 °C and keeping ΔT at 250 °C. Burns and Bright (1998) have shown that similar Au/Si layered structures undergo thermally induced damage at tempera-

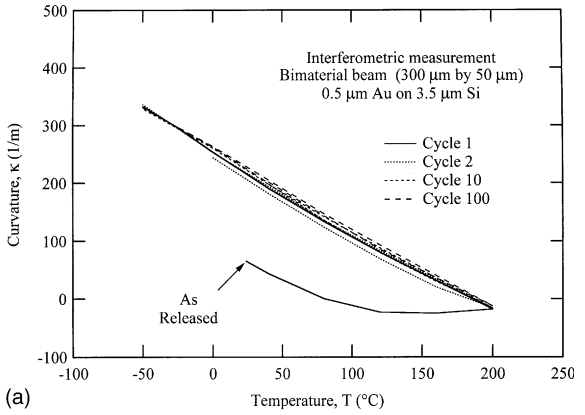

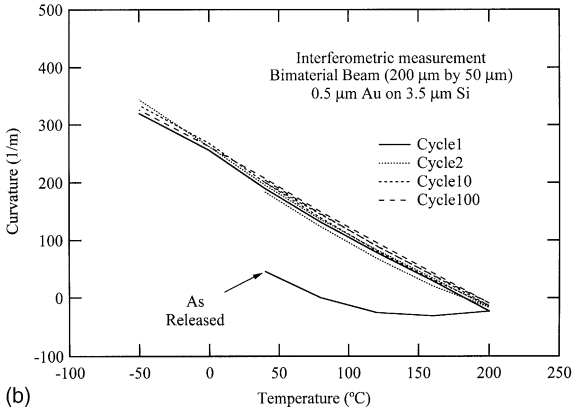

Fig. 10. Thermal cycling response of (a) a 300 μm by 50 μm beam and (b) a 200 μm by 50 μm beam. Test parameters: $\Delta T = 250$ °C, $T_m = 75$ °C.

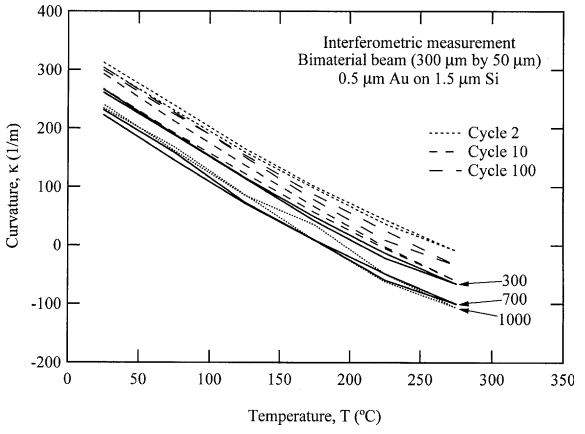

Fig. 11. Thermal cycling response of a 300 μm by 50 μm beam. Test parameters: $\Delta T = 250$ °C, $T_m = 150$ °C.

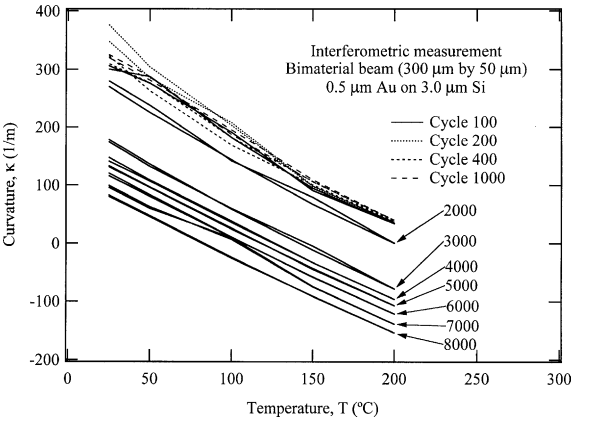

Fig. 12. Thermal cycling response of a 300 μm by 50 μm beam. Test parameters: $\Delta T = 175$ °C, $T_m = 112.5$ °C.

tures 250 °C and higher. This type of damage may contribute to the trends seen in Fig. 11. After 100 cycles, the thermomechanical response has shown a significant downward shift towards smaller curvatures, and at 1000 cycles the reflectivity of gold surface had degraded so as to make interference measurements impractical. This surface reflectivity degradation is a result of the thermally induced damage mentioned previously. A final thermal cycling result is presented in Fig. 12 for $\Delta T = 175$ °C and $T_m = 112.5$ °C. This cycling scheme produced a slower degradation response than Fig. 11. The sample lasted more 8000 cycles with continually decreasing curvature before the experiment was terminated.

4. Discussion

To design functional and reliable multi-layer MEMS structures, it is necessary to understand and predict their thermomechanical response for a variety of possible loading paths and structure geometries. The present results provide a preliminary investigation into the effects of layer thickness, plate geometry, thermal path, and repeated cycling on the thermomechanical response of layered Au–Si MEMS structures. Within this discussion we shall provide explanations for some of the observed results and future paths for elucidating unclear behaviors.

Multi-layered Au–Si square plates with a comparable in-plane x and y dimensions demonstrate a non-linear curvature versus temperature response. Smaller plates exhibit a spherical out-of-plane deformation pattern with equivalent curvatures in the x and y directions. Larger plates show equivalent x and y curvatures for relatively small curvatures, however, the x and y curvatures eventually bifurcate resulting in a buckled plate structure. Structures with a higher in-plane aspect ratio do not show a noticeable size effect or bifurcation. Finite element modeling results have proven that the non-linear curvature effects are geometrical in nature. In the finite element model, the bifurcation must be seeded by introducing a material or geometrical imperfection (Dunn et al., 2001, 2002).

Existing finite element and constitutive models are capable of predicting the curvature–temperature response of the MEMS plates for one stabilized thermomechanical cycle (Fig. 8, Dunn et al., 2001, 2002). The reason that the aforementioned finite element model shows good correlation with experiments for a *single stabilized* thermomechanical cycle is because micro-structural changes are negligible over a single stabilized cycle and non-linear elastic constitutive relationships are valid. Predicting the behavior of an as-released structure (Figs. 6 and 7), or a structure subjected to thermal hold periods (Fig. 9) or repeated cycles (Figs. 10–12) requires a constitutive damage modeling approach. Although such frameworks are standard for macroscale material systems, it is not certain at this time that these models can be extrapolated to these small scales without modification.

The first thermomechanical cycle of as-released structures differs considerably than subsequent cycles. During an initial heating cycle, significant energy dissipation occurs through one or many inelastic deformation mechanisms. This observation is clear from the open hysteresis loops in Fig. 7, which are analogous to an elastic–plastic stress–strain curve with intermittent unloading segments (Zhang and Dunn, 2003). As mentioned in the introduction the inelastic behavior in thin films on thick substrates in micro-electronics has been rationalized as plastic flow, diffusion, grain growth, or dislocation creep. Detailed microscopy work or further experimentation must be completed in multi-layer MEMS structures to fully determine the inelastic deformation mechanisms controlling the response of the as-released Au–Si structures. Such investigations are part of the present work and results will be presented in due course. We do not believe that the deformation mechanism can be simply explained by plasticity since the stresses in the films are very small at the onset of the inelastic deformation. For example, upon cooling to room temperature from 125 °C, the stresses in the Au film in the structures in Fig. 7 are approximately 75 MPa. Near the zero curvature values in Fig. 7, the stresses in the films are on the order of 10s of MPa.

The preliminary thermal cycling results presented here show that the curvature–temperature response depends on the number of applied thermal cycles. Based on Fig. 11, a structure cycled at a relatively high mean (or max) temperature will show a downward ratcheting leading to excessive surface roughening. Fig. 12 shows the evolution of the thermomechanical response when the sample is not subjected to temperatures above 200 °C during cycling. The sample degrades much slower, and the thermomechanical response also ratchets towards a lower curvature value. It appears that a different degradation mechanism is operating in this regime compared to the higher temperature regime. Microstructural observations and modeling are needed to fully understand this evolutionary behavior during cycling. Moreover, further experimentation is necessary to clarify and quantify the role of the temperature range versus the mean temperature on the cyclic response. With the aforementioned micro-structural and experimental information, mechanism-based models of the cyclic response can be developed as a step towards new multi-layer MEMS design tools.

5. Conclusions

1. Bi-layer Au–Si MEMS structures exhibit a non-linear temperature–curvature relationship during a temperature change due to thermal expansion coefficient mismatch between the two thin layers. Square plate structures show a size effect of the curvature–temperature response,

and larger plates show a tendency to buckle. Beam-like structures do not exhibit a length effect.
2. Bi-layer Au–Si MEMS structures show a relaxation or curvature (creep) when subjected to a thermal hold period.
3. The first thermal cycle of as-released Au–Si bi-layer MEMS differs considerably compared to subsequent cycles. Beam-like samples cycled between two temperatures showed significant ratcheting toward a lower curvature as a function of the number of cycles.
4. Future work on bi-layer MEMS structures must focus on understanding the mechanisms of deformation during creep and thermal cycling. Previous research on thin films in microelectronics may not trivially extend to MEMS structures due to the completely different coupling between temperature, induced curvature, and stress in the two applications.

Acknowledgements

This work is supported by grants from DARPA and the NSF/Sandia life-cycle engineering program. We thank Chris Parks at Maxtor for assisting with FIB images. Undergraduate CU student Mike Hulse is thanked for his help with data reduction and measurements.

References

Burns, D.M., Bright, V.M., 1998. Optical power induced damage to microelectromechanical mirrors. Sens. Actuator A: Phys. 70, 6.

Dunn, M.L., Zhang, Y., Bright, V., 2001. Deformation and structural stability of gold/polysilicon plate structures subjected to thermal loading. In: Muhlstein, C., Brown, S.B. (Eds.), ASTM STP 1413. American Society for Testing and Materials, West Conshohocken, PA.

Dunn, M.L., Zhang, Y., Bright, V., 2002. Deformation and structural stability of layered plate microstructures subjected to thermal loading. J. Microelectromech. Syst. 11, 372.

Evans, A.G., He, M.Y., Hutchinson, J.W., 1997. Effect of interface undulations on the thermal fatigue of thin films and scales on metal substrates. Acta Mater. 45, 3543.

Finot, M., Suresh, S., 1996. Small and large deformation of thick and thin film multilayers: effect of layer geometry, plasticity, and compositional gradients. J. Mech. Phys. Solids 44, 683.

Freund, L.B., 2000. Substrate curvature due to thin film mismatch strain in the nonlinear deformation range. J. Mech. Phys. Solids 48, 1159.

Harris, K.E., King, A.H., 1998. Direct observation of diffusional creep via TEM in polycrystalline thin films of gold. Acta Mater. 46, 6195.

He, M.Y., Evans, A.G., Hutchinson, J.W., 1997. The ratcheting of compressed thermally grown thin films on ductile substrates. Acta Mater. 48, 2593.

Hommel, M., Kraft, O., Arzt, E., 1999. A new method to study cyclic deformation of thin films in tension and compression. J. Mater. Res. 14, 2373.

Keller, R.-M., Baker, S.P., Arzt, E., 1999. Stress–temperature behavior of unpassivated thin copper films. Acta Mater. 47, 415.

Koike, J., Utsunomiya, S., Shimoyama, Y., Maruyama, K., Oikawa, H., 1998. Thermal cycling fatigue and deformation mechanism in aluminum alloy thin films on silicon. J. Mater. Res. 13, 3256.

Koester, D.A., Mahadevan, R., Hardy, B., Markus, K.W., 2001. MUMPs Design Rules. Cronos Integrated Microsystems, A JDS Uniphase Company., Available from: http://www.memsrus.com/cronos/svcsrules.html.

Leung, O.S., Munkholm, A., Brennan, S., Nix, W.D., 2000. A search for strain gradients in gold thin films on substrates using X-ray diffraction. J. Appl. Phys. 88, 1389.

Miller, D.C., Zhang, W.G., Bright, V.M., 2001. Micromachined, flip-chip assembled, actuatable contacts for use in high density interconnection in electronics packaging. Sens. Actuator A: Phys. 89, 76.

Nix, W.D., 1989. Mechanical properties of thin films. Metall. Trans. A 20, 2217.

Read, D.T., 1998. Tension–tension fatigue of copper thin films. Int. J. Fatigue 20, 203.

Salamon, N.J., Masters, C.B., 1995. Bifurcation in isotropic thin film/substrate plates. Int. J. Solids Struct. 32, 473.

Schwaiger, R., Kraft, O., 1999. High cycle fatigue of thin silver films investigated by dynamic microbeam deflection. Scr. Mater. 41, 823.

Shen, Y.-L., Suresh, S., 1995. Thermal cycling and stress relaxation response of Si–Al and Si–Al–SiO_2 layered thin films. Acta Metall. Mater. 43, 3915.

Stoney, G.G., 1909. The tension of metallic films deposited by electrolysis. Proc. R. Soc. London A 82, 172.

Thouless, M.D., Gupta, J., Harper, J.M.E., 1993. Stress development and relaxation in copper films during thermal cycling. J. Mater. Res. 8, 1845.

Zhang, Y., Dunn, M.L., 2001. Stress relaxation of gold/polysilicon layered MEMS microstructures subjected to thermal loading. In: Proceedings of the MEMS Symposium, ASME International Mechanical Engineering Congress and Exposition 3, p. 149.

Zhang, Y., Dunn, M.L., 2003. Deformation of multilayer thin film microstructures during post-release cyclic thermal loading: implications for MEMS design, packaging, and reliability. Submitted for publication.